Chin. J. Astron. Astrophys. Vol. 2 (2002), No. 1, 17–32
(*http://www.chjaa.org* or *http://chjaa.bao.ac.cn*)

Chinese Journal of
Astronomy and
Astrophysics

Abundance Gradient from Open Clusters and Implications for the Galactic Disk Evolution

Jin-Liang Hou ⋆, Rui-Xiang Chang and Li Chen

Shanghai Astronomical Observatory, Chinese Academy of Sciences, Shanghai 200030
National Astronomical Observatories, Chinese Academy of Sciences, Beijing 100012

Received 2001 June 2; accepted 2002 January 6

Abstract We compile a new sample of 89 open clusters with ages, distances and metallicities available. We derive a radial iron gradient of about -0.099 ± 0.008 dex kpc^{-1}(unweighted) for the whole sample, which is somewhat greater than the most recent determination of oxygen gradient from nebulae and young stars. By dividing the clusters into age groups, we show that the iron gradient was steeper in the past and has evolved slowly in time. Current data show a substantial scatter of the cluster metallicities indicating that the Galactic disk has undergone a very rapid, inhomogeneous enrichment. Also, based on a simple, but quite successful model of chemical evolution of the Milky Way disk, we make a detailed calculation of the iron abundance gradient and its time evolution. The predicted current iron gradient is about -0.072 dex kpc^{-1}. The model also predicts a steady flattening of the iron gradient with time, which agrees with the result from our open cluster sample.

Key words: open clusters: abundances – Galaxy: formation – Galaxy: evolution

1 INTRODUCTION

Radial abundance gradient along the Galactic disk constitutes one of the most important observational constraints for models of the evolution of the Galactic disk. The existence of such a gradient is now well established, through radio and optical observations of HII regions, disk stars, planetary nebulae (see Henry and Worthey 1999 for a detailed review) and open clusters (Friel 1995, 1999). An average gradient of $\mathrm{dlog(X/H)/d}R \sim -0.06$ dex kpc^{-1} is observed in the Milky Way for most of the elements, e.g., O, S, Ne, Ar and Fe, while the gradients for C and N are, perhaps, slightly larger (Smartt 2000).

An equally important, but still unsettled question is the history of abundance gradient: was it steeper or flatter in the past? This is crucial in constraining the initial conditions and evolutions of the gas and stars in the Galactic disk, the infall history, pre-enrichment, coupling between the halo and disk evolutions etc. Different predictions are made by various current models of Galactic chemical evolution, although most of them claim that they could

⋆ E-mail: hjlyx@center.shao.ac.cn

reproduce the majority of observational data for both the solar neighborhood and the whole disk. The models of Prantzos & Aubert (1995), Mollá et al. (1997), Allen et al. (1998), Boissier & Prantzos (1999) and Hou et al. (2000) suggest a flattening of the gradient in time, while the models of Tosi (1988), Samland et al. (1997) and Chiappini et al. (1997, 2001) support an evolution in the opposite direction. The situation is not settled observationally either. The estimated ages of planetary nebulae (PN) of various types (PNI, PNII, PNIII) span a large fraction of the age of the Galaxy. Observations of the abundances of these objects across the Milky Way disk could, in principle, provide some information on the past history of the abundance gradient (Maciel & Koppen 1994, Maciel & Quireza 1999). In a recent work, Hou et al. (2000) have made a detailed analysis for the O, Ne, S and Ar gradient evolution based on the PN data of Maciel & Quireza (1999). It was shown that there exists fairly good agreement between theory and observations on all the properties of the observed abundance profiles (absolute values, gradient and scatter) for O, S, Ne and Ar. The model suggests that the abundance gradients were steeper in the early epoch. However, the large scatter in the adopted data does not allow a conclusion on the temporal variation of the gradients, although a possible steepening tendency in time was suggested by Maciel & Quireza (1999). Nevertheless, PNs suffer from large uncertainties concerning their progenitor masses and lifetimes and their distances from the Galactic center.

On the other hand, open clusters (OCs) have long been used to trace the structure and evolution of the Galactic disk (Friel 1995). Because they could be relatively accurately dated and we can see them to large distances, their [Fe/H] abundances make up an excellent trace to the abundance gradient along the Galactic disk as well as to many other important disk properties, such as Age-Metallicity Relation (AMR), the disk age and so on. Our Galactic chemical evolution model was very successful in explaining the abundance profiles of many elements (including O, Al, Si, S, Ne, and Ar) along the galactic disk. It should be important to further explore the iron abundance profile along the Galactic disk. Our specific purpose in this paper is to trace the time variation of iron abundance based on a relatively large OC samples and to make a detailed comparison with the model results. Our sample contains more objects compared with previous similar works, and should therefore be more significant statistically.

At this point, one might ask whether the field disk populations are also able to trace the disk evolution. Indeed, the extensive studies by Edvardsson et al. (1993) and recently by Chen et al. (2000), concentrated on disk F, G stars, showed an overall radial gradient that is nearly independent of age. This was further confirmed by the recent study of Corder & Twarog (2001). These results were based on stars mainly restricted to the solar neighborhood. A more detailed analysis for the disk iron gradient was given by Cui et al. (2000) on the basis of 1302 field stars with high resolution proper motion and parallax data from Hipparcos satellite. They derived an iron radial gradient of -0.057 dex kpc^{-1} within galactocentric distance from 8.5 kpc to 17 kpc. However, it is difficult to extract any clear gradient evolution from those statistics. Moreover, results from those studies were strongly affected by selection effects and the individual distances used depend heavily on the adopted model of Galaxy gravitational potential, hence are much less reliable than the cluster distances.

This paper is organized as follows: in Section 2, we summarize the current observational status of open cluster gradients; we then present a combined open cluster sample in Section 3 and, on the basis of sub-samples, explore the iron gradient evolution with time. Our basic model is introduced in Section 4.1, and Section 4.2 discusses in detail the comparison between our model predictions and the observations. Finally, a brief summary is given in Section 5.

2 IRON GRADIENT FROM OPEN CLUSTERS

Since the pioneering work by Janes (1979) concerning the iron gradients from open clusters, a number of authors have published results on the galactic disk gradients using the spectroscopic and photometric indices of stellar populations in open clusters (Panagia & Tosi 1981, Cameron 1985, Janes et al. 1988, Friel & Janes 1993, hereafter FJ93, Thogerson et al. 1993, Friel 1995, hereafter F95, Piatti, Claria & Abadi 1995, hereafter PCA95, Twarog, Ashman & Anthony-Twarog 1997, hereafter TAA97, Carraro, Ng & Portinari 1998, hereafter CNP98, Ying 1998, Friel 1999). The derived gradients vary between $-0.05 \sim -0.133$ dex kpc^{-1}over a galactocentric distance from 6 to 16 kpc (see details in Hou & Chang 2001). Table 1 summarises the iron gradients derived from available data.

Table 1 [Fe/H] Gradient from Open Clusters

R_g (kpc)	Age (Gyr)	Gradient (dex kpc^{-1})	No.	Ref.
7.5–16.2	> 0.70	–0.060±0.010	41	[1]
6.8–13.4	0.01–7.10	–0.107±0.009	79	[2]
7.6–16.0	0.60–9.00	–0.085±0.008	37	[3]
6.4–15.0	0.10–8.00	–0.067±0.008	76	[4]
6.8–13.4	0.10–8.00	–0.070±0.010	63	[5]
7.5–16.0	> 0.80	–0.091±0.014	44	[6]
7.1–15.4	0.20–8.00	–0.097±0.017	29	[7]
7.9–14.5	0.80–8.00	–0.088±0.017	24	[8]
	< 0.20	–0.078		
6.5–13.5	mixed	–0.113	87	[9]
	> 0.20	–0.140		
6.9–10.9	mixed	–0.110±0.020	38	[10]
8.5–12.1	< 1.00	–0.095±0.034	20	[11]
8.0–14.0	mixed	–0.050±0.010	41	[12]
6.5–16.0	0.01–11.0	–0.099±0.008 (unweighted)	89	this paper
		–0.080±0.001 (weighted)		

References: [1] Friel 1999; [2] Ying 1998; [3] Carraro, Ng & Portinari 1998 [CNP98]; [4] Twarog, Ashman & Anthony-Twarog 1997 (TAA97); [5] Piatti, Claria & Abadi 1995 (PCA95); [6] Friel 1995 (F95); [7] Thogerson, Friel & Fallon 1993; [8] Friel & Janes 1993 (FJ93); [9] Janes et al. 1988; [10] Cameron 1985; [11] Panagia & Tosi 1981; [12] Janes 1979

Table 1 indicates that the [Fe/H] gradients from the various samples are within $-0.06 \sim -0.11$ dex kpc^{-1}, while for the time evolution, open clusters alone show some indications of time flattening when the clusters are divided into sub-samples of different ages. But the sub-samples are too small and make the result statistically uncertain. In any case, our current knowledge on the iron gradient as derived from open clusters is far being clear. When comparing these results with those from young objects such as HII regions and early-B giants, we must note that the open clusters can be as old as 8 Gyr, so that they do not trace the young component of the galactic disk.

3 NEW OC SAMPLE AND GRADIENT EVOLUTION

If we compare [Fe/H] abundance gradient of open clusters with the [O/H] gradient derived from HII regions, early B stars and PNII objects, the gradient seems to have remained roughly constant in the past several Gyr. However, such a comparison should be taken with care because iron and oxygen have different nucleosynthesis origins. Iron is produced mainly in SNIa and in partly SNII, while oxygen has its origin in SNII. This being so, they must have had distinctly different evolutionary histories in the Galaxy. Due to the lack of oxygen abundance in older clusters, it is better to compare the iron gradients among various groups of open clusters with different ages in order to trace the time evolution. At present, several samples of open clusters are available, each has a limited number of clusters (see Table 1). So we wanted to see if we could compile a relatively larger sample from those although there might exist different scales of ages, metallicities, and distances among the different authors. In general, the scatter in the abundance due to differences in the adopted techniques and atomic data is smaller than the observational uncertainties. Therefore, we believe that a combination of the different samples could still provide statistically meaningful results. Especially, as there are some clusters common to different samples, we can make cross checks to see if there are systematic differences.

Our following analysis is based on four samples (see Table 1): CNP98, TAA97, PCA95, and F95 & FJ93. The detailed descriptions of age, distance and metallicity calibration can be found in the relevant papers, here we only concentrate on the overall statistical properties of these parameters. Before combining the samples, we have to make a statistical comparison among the data to see if there are significant differences.

Since the majority of the clusters are based on Lyngå (1987) Catalog, the distances are exactly correlated among the four samples. As to the metallicity, three of the samples, CNP98, PCA95 and F95 are well correlated, and they all have some biases as compared to the TAA97 sample. In fact, in their calibrations, PCA95 and F95 have made use of many of the same field stars, and CNP98 has adopted the same metallicity scale as F95 and FJ93. The abundances of TAA97 are systematically a little larger than the others. This resulted from a small adjustment in the abundance calibration in TAA97 whose authors suggested that the metallicity zero-point used in F95 and FJ93 may be in error. The difference is, however, small and it should not have any significant influence on the statistical results (within 2σ). There also exists age difference in the different samples. The ages in F95 are based on the MAI (Morphological Age Index) of Janes & Phelps (1994). The MAI was only intended to provide a relative age ranking of clusters, and not as a true age, but does not matter in the present paper, for we only need relative age differences among the clusters in order to investigate the time evolution of the gradient.

Therefore, we can recompile a new sample in which the cluster parameters, the distance, abundance and age, are determined by averaging over the above samples for common objects. As a result, the combined sample contains 89 open clusters with galactocentric distances between 6.5 kpc and 16 kpc and ages between 0.02 Gyr and 11 Gyr. The whole sample is given in Table 2. Cross checks for the common objects between the mean sample and the four individual samples are given in Figures 1, 2 and 3. It can be seen that they are well correlated statistically (95.4% confidential level within 2σ).

Table 2 Abundances, Ages and Distances of the Mean Sample

No.	name	R_{GC} (kpc)	[Fe/H]	Age (Gyr)	Ref.	$\sigma_{[Fe/H]}$
1	NGC 188	9.352	−0.072	6.567	1,2,3,4	0.161
2	NGC 752	8.757	−0.157	1.767	1,2,3,4	0.073
3	NGC 1193	12.737	−0.430	4.950	1,2,4	0.206
4	NGC 1245	11.095	0.140	0.900	2,4	0.100
5	NGC 1342	8.990	−0.240	0.300	3	0.120
6	NGC 1545	9.230	−0.060	0.190	1,3	0.09
7	NGC 1662	8.870	−0.060	0.300	1,3	0.014
8	NGC 1817	10.270	−0.350	1.050	1,2,4	0.045
9	NGC 2099	9.850	0.135	0.300	1,3	0.099
10	NGC 2112	9.265	−0.315	4.000	1,4	0.09
11	NGC 2141	12.687	−0.347	2.650	1,2,4	0.111
12	NGC 2158	12.578	−0.265	1.573	1,2,3,4	0.195
13	NGC 2168	9.355	−0.220	0.110	1,3	0.09
14	NGC 2204	11.510	−0.472	2.320	1,2,3,4	0.270
15	NGC 2243	11.057	−0.553	5.033	1,2,3,4	0.214
16	NGC 2251	9.950	−0.125	0.300	1,3	0.072
17	NGC 2287	8.995	−0.045	0.100	1,3	0.061
18	NGC 2301	9.190	0.035	0.110	1,3	0.06
19	NGC 2324	11.290	−0.310	0.900	4	0.140
20	NGC 2335	9.310	−0.005	0.160	1,3	0.09
21	NGC 2360	9.263	−0.190	1.450	1,3,4	0.076
22	NGC 2420	10.462	−0.385	2.967	1,2,3,4	0.101
23	NGC 2423	9.083	0.070	0.575	4	0.072
24	NGC 2437	9.420	0.065	0.300	1,3	0.09
25	NGC 2477	8.967	−0.027	0.800	1,2,4	0.121
26	NGC 2482	8.965	0.125	0.400	1,3	0.045
27	NGC 2489	9.165	0.090	0.240	1,3	0.01
28	NGC 2506	10.577	−0.475	2.800	1,2,3,4	0.110
29	NGC 2516	8.480	0.040	0.110	1,3	0.03
30	NGC 2527	8.765	−0.085	1.000	1,3	0.09
31	NGC 2539	9.280	0.155	0.660	1,3	0.085
32	NGC 2546	8.830	−0.010	0.040	1,3	0.13
33	NGC 2547	8.550	−0.185	0.060	1,3	0.09
34	NGC 2548	8.900	0.045	0.300	1,3	0.022
35	NGC 2567	9.210	−0.060	0.070	1,3	0.225
36	NGC 2632	8.635	0.117	0.780	1,3,4	0.072
37	NGC 2660	9.097	−0.083	1.060	1,2,3,4	0.175
38	NGC 2682	9.083	−0.061	5.250	1,2,3,4	0.110
39	NGC 2972	8.490	−0.080	0.400	1,3	0.014
40	NGC 3114	8.330	−0.060	0.110	1,3	0.146
41	NGC 3532	8.350	−0.040	0.350	1,3	0.098
42	NGC 3680	8.290	−0.145	2.433	1,2,3,4	0.088
43	NGC 3960	7.967	−0.228	0.800	1,2,3,4	0.099
44	NGC 4349	7.770	−0.090	0.220	1,3	0.064
45	NGC 5138	7.495	0.150	0.150	1,3	0.05
46	NGC 5316	7.745	0.055	0.190	1,3	0.139
47	NGC 5822	7.915	−0.105	0.983	1,2,3,4	0.151
48	NGC 6067	6.805	0.065	0.080	1,3	0.076
49	NGC 6134	7.720	0.190	0.630	1,3	0.104
50	NGC 6208	7.580	0.015	1.000	1,3	0.072
51	NGC 6253	6.600	0.280	4.000	2,3	0.03
52	NGC 6259	7.070	0.015	0.220	1,3	0.127
53	NGC 6281	7.920	0.000	0.220	1,3	0.150
54	NGC 6425	7.700	0.080	0.060	1,3	0.09
55	NGC 6475	8.240	0.050	0.220	1,3	0.09
56	NGC 6494	7.820	0.110	0.220	1,3	0.175
57	NGC 6633	8.230	−0.010	0.660	1,3	0.064
58	NGC 6705	6.930	0.175	0.200	1,4	0.040
59	NGC 6791	8.183	0.163	8.750	1,2,4	0.194
60	NGC 6819	8.187	0.057	2.575	1,2,4	0.121
61	NGC 6939	8.737	−0.073	1.800	1,2,4	0.117
62	NGC 6940	8.240	−0.003	0.700	1,2,4	0.117
63	NGC 7142	9.557	0.013	4.650	1,2,4	0.063
64	NGC 7209	8.655	−0.025	0.300	1,3	0.05
65	NGC 7789	9.445	−0.205	1.683	1,2,3,4	0.145
66	Berk17	11.160	−0.290	10.800	2,4	0.13
67	Berk19	13.300	−0.500	3.400	2,4	0.10
68	Berk20	16.145	−0.750	3.950	2,4	0.21
69	Berk21	14.385	−0.970	2.800	2,4	0.218
70	Berk31	12.310	−0.500	3.750	2,4	0.16
71	Berk32	11.650	−0.580	5.100	2,4	0.10
72	Berk39	11.757	−0.267	6.850	2,4	0.08
73	Cr261	7.545	−0.140	8.250	2,4	0.14
74	HAF8	9.790	0.060	0.500	1,3	0.072
75	HAR5	8.015	−0.165	0.040	1,3	0.09
76	HYADES	8.543	0.160	0.780	1,3,4	0.036
77	IC166	11.270	−0.273	1.175	1,2,4	0.233
78	IC2714	8.075	0.000	0.320	1,3	0.108
79	IC4651	7.730	−0.037	1.933	1,2,3,4	0.105
80	IC4756	8.180	−0.140	0.900	1,4	0.03
81	King5	10.420	−0.380	0.850	2,4	0.20
82	King8	12.780	−0.430	0.800	1,4	0.09
83	King11	10.095	−0.360	6.150	2,4	0.14
84	LO807	8.080	−0.130	0.000	1,3	0.09
85	MEL66	9.690	−0.452	5.153	1,2,3,4	0.148
86	PI4	8.605	−0.125	0.020	1,3	0.120
87	RUP18	9.090	0.035	0.130	1,3	0.09
88	RUP46	8.910	−0.130	3.160	3	0.18
89	TOM2	14.643	−0.470	2.125	1,2,4	0.18

Ref: 1. Twarog et al. 1997 (TAA97, cluster ages are not available); 2. Carraro et al. 1998 (CNP98); 3. Piatti et al. 1995 (PCA95); 4. Friel & Jane 1993, Friel 1995 (F95).

Figure 4 shows the plots for the combined sample as well as the four original samples. Note that in F95, there are 44 objects, while in the plot we have 48, the four additional clusters are NGC 2112, NGC 6253, NGC 6705 and Berk 19, from FJ93 and Thogersen et al. (1993). The dash line is the unweighted least square fitting of the data. The resulting gradient is about -0.099 ± 0.008 dex kpc^{-1}. The weighted fitting results in a value of -0.080 ± 0.001 dex kpc^{-1}.

Our new sample clearly shows a linear gradient for the range of galactocentric distance between 6 and 16 kpc; however, this was questioned by Twarog, Ashman & Anthony-Twarog (1997). They found that the metallicity distribution of clusters with galactocentric distance is best described by two distinct zones, with a sharp discontinuity at $R_{\rm GC} = 10$ kpc. Between $R_{\rm GC} = 6.5$ kpc and 10 kpc, the clusters have a mean metallicity 0.0 dex with, at best, weak evidence for a shallow gradient over this range, while those beyond 10 kpc have a mean value about -0.30 dex. TAA97 puts forth an alternative description, a step function, for the radial abundance distribution of the open clusters. This two-step distribution seems quite similar with the nebula results of Simpson et al. (1995). However, a careful check with the cluster ages

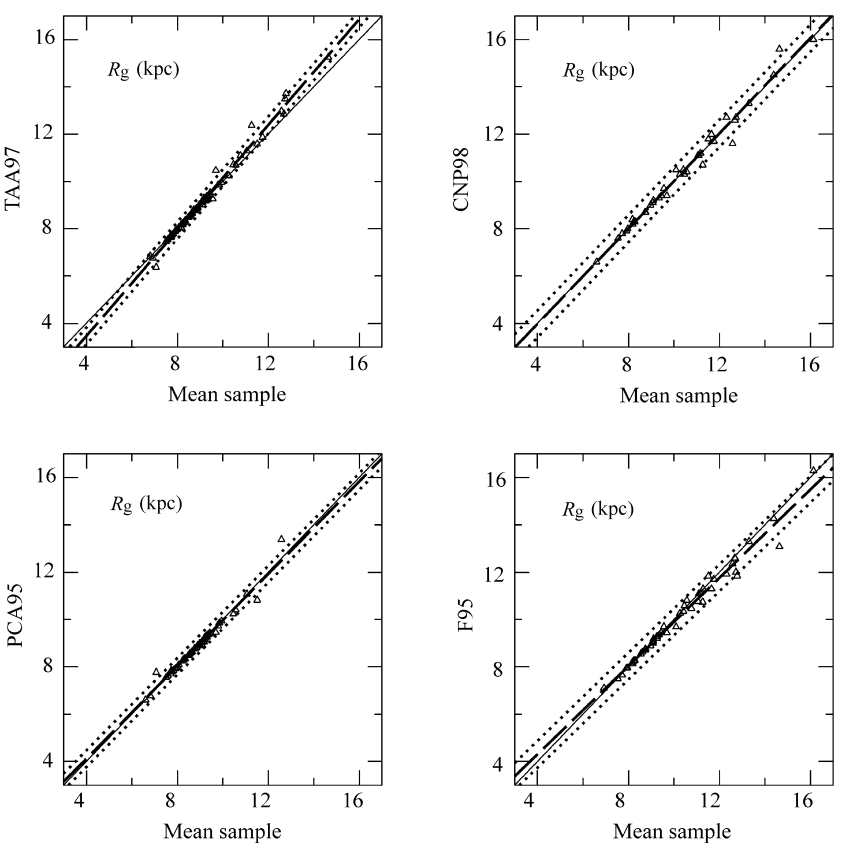

Fig. 1 Comparison of the distances of the mean sample and the four original samples for the common clusters. Dash lines are the least-square fitting, dot lines are the 2σ limits. The difference is small at the 95.4% confidential level.

shows that the sample inside 10 kpc is heavily weighted towards clusters younger than 1 Gyr, while the outer clusters are predominantly older clusters (see Figure 6). Neglecting this two-step phenomena, a least square fitting results in a gradient about -0.067 dex kpc^{-1} between 6 and 15 kpc if cluster BE21 was excluded because both the metallicity and distance of this object are quite uncertain.

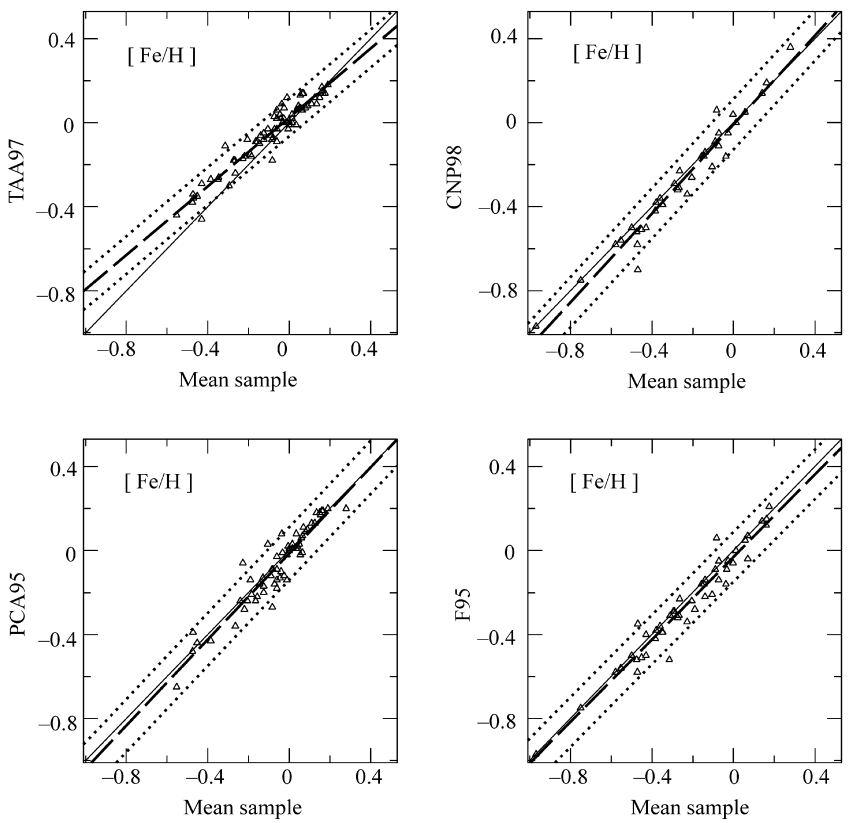

Fig. 2 Same as Figure 1, but for metallicity.

Since the clusters extend over a large range of ages (from 0.1 Gyr to 11 Gyr), we doubt that this could really reflect the abundance history of the disk (however, such a gradient was always quoted by many authors). An alternative is to divide the clusters into age groups, and explore the gradient differences among the different groups. In so doing, it should be emphasized, first, that the separation should not result in groups of very different sizes in order to keep them statistically comparable; then that there could be some difference between dividing into two or three groups that might reflect the significant evolution of the Galactic disk. With this in mind, we made two tests, one with the clusters divided into two groups, one into three groups. From the first we examine the gradient differences between older and younger clusters, while from the second we explore further the behavior of intermediate age clusters.

Table 3 gives the results for the first case, where the last two columns are the correlation coefficients of the least square fitting and the corresponding confidential levels. Note that we only give the gradients of unweighted fitting, the weighted fitting gives similar values. However, since the data error systems among different sub-samples are quite different, the given final errors in the combined sample are merely for illustration purpose. The weighting factors based on those errors cannot reflect the real situation.

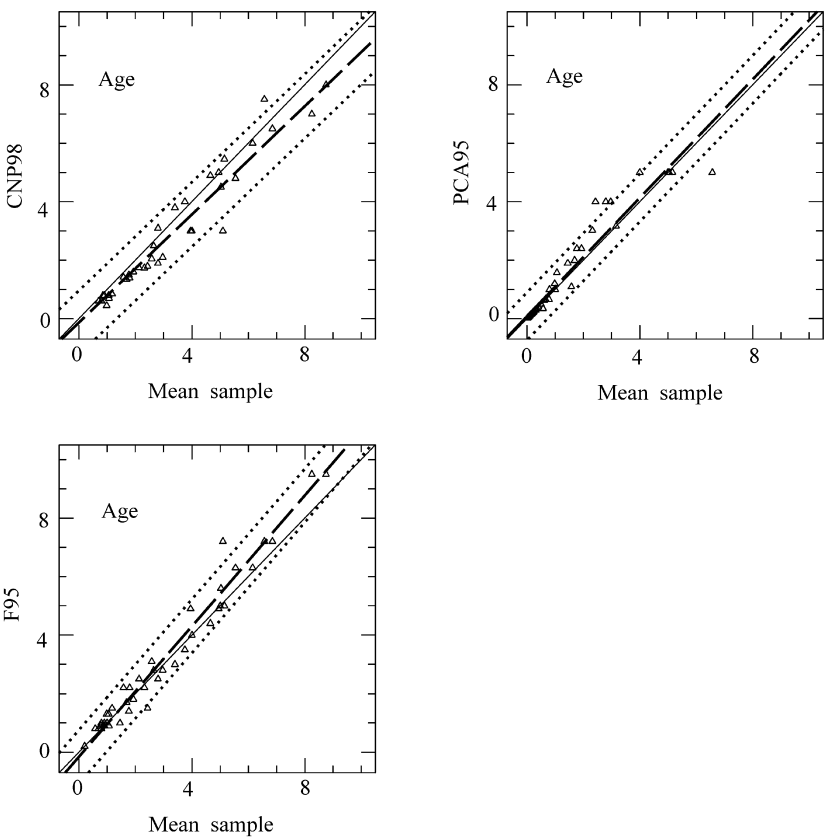

Fig. 3 Same as Figure 1, but for age (note: cluster ages are not available for TAA97)

Clearly, whatever value we select for the age bin t between 0.85 (typical age of the Hyades cluster) and 2.0 Gyr, the older clusters always show a much steeper gradient than do the younger clusters. This implies that, as a general tendency, the gradient becomes flatter during the evolution of the disk. This agrees with the earlier results of Janes et al. (1988) and the recent statistics of Ying (1998) (see Table 1).

Now, we turn to the case of three age bins. The results are given in Table 4. Again, we see that in the selected age bins, the gradient is the greatest in the older group. We notice that for the young age bin, the correlation coefficient is not always significant, because the younger clusters are heavily concentrated in the solar neighborhood. From Figures 4 and 6, we see that

there are only four young clusters around 11 kpc, much less than in the solar neighborhood, due to the current observational limitation of young clusters, and we should bear this in mind when judging the gradient from young clusters. However, it is obvious that the gradient is systematically smaller in the intermediate than the older group. The fact is inconsistent with CNP98, who suggested that the middle epoch clusters seem to display a steepening of the gradient. In order to have a more reliable gradient, it is necessary to have more data of young clusters located in the outer part of the disk.

Table 3 Iron Gradients (unweighted fit) for Two Age Bins

Age bin (Gyr)	$R_{\rm GC}$ (kpc)	Gradient (dex kpc^{-1})	No. of OCs	$R_{\rm coe}$	C.L.
$t < 0.80$	6.8–10.0	–0.027±0.022	44	0.29	95 %
$t \geq 0.80$	6.6–16.1	–0.092±0.011	45	0.79	>99 %
$t < 0.85$	6.8–12.8	–0.055±0.018	47	0.41	>99 %
$t \geq 0.85$	6.6–16.1	–0.094±0.011	42	0.79	>99 %
$t < 0.90$	6.8–12.8	–0.065±0.018	48	0.47	>99 %
$t \geq 0.90$	6.6–16.1	–0.094±0.011	41	0.80	>99 %
$t < 1.00$	6.8–12.8	–0.055±0.017	52	0.42	>99 %
$t \geq 1.00$	6.6–16.1	–0.097±0.011	37	0.84	>99 %
$t < 2.00$	6.8–12.8	–0.064±0.014	63	0.51	>99 %
$t \geq 2.00$	6.6–16.1	–0.101±0.013	26	0.83	>99 %
$t < 3.00$	6.8–14.6	–0.092±0.011	71	0.71	>99 %
$t \geq 3.00$	6.6–16.1	–0.101±0.016	18	0.84	>99 %
global	6.6–16.1	–0.099±0.008	89	0.78	>99 %

Table 4 Iron Gradients (unweighted fit) for Three Age Bins

Age bin (Gyr)	$R_{\rm GC}$ (kpc)	Gradient (dex kpc^{-1})	No. of OCs	$R_{\rm coe}$	C.L.
$t < 0.30$	6.8–9.40	–0.055±0.025	25	0.42	>95 %
$0.30 \leq t < 1.00$	7.7–12.8	–0.062±0.026	27	0.43	>99 %
$t \geq 1.00$	6.6–16.1	–0.097±0.011	37	0.84	>99 %
$t < 0.60$	6.8–10.0	–0.027±0.021	38	0.21	<95 %
$0.60 \leq t < 2.50$	7.6–14.6	–0.074±0.016	28	0.67	>99 %
$t \geq 2.50$	6.6–16.1	–0.110±0.015	23	0.85	>99 %
$t < 0.80$	6.8–10.0	–0.027±0.022	44	0.19	<95 %
$0.80 \leq t < 3.00$	7.6–14.6	–0.085±0.015	27	0.74	>99 %
$t \geq 3.00$	6.6–16.1	–0.101±0.017	18	0.84	>99 %
$t < 1.00$	6.8–12.8	–0.055±0.017	52	0.42	>95 %
$1.00 \leq t < 3.00$	7.6–14.6	–0.094±0.016	19	0.84	>99 %
$t \geq 3.00$	6.6–16.1	–0.101±0.017	18	0.84	>99 %
$t < 1.00$	6.8–12.8	–0.055±0.017	52	0.42	>95 %
$1.00 \leq t < 4.50$	6.6–16.1	–0.095±0.011	25	0.88	>99 %
$t \geq 4.50$	7.5–12.7	–0.109±0.032	12	0.71	>99 %
global	6.6–16.1	–0.099±0.008	89	0.78	>99 %

Though the combined sample is not complete and accurate enough, the statistical results should be reliable since there exists a good cross correlation among the four samples we used. Our conclusion is that, on the basis of current open clusters data, the iron gradient becomes shallower during the Galactic disk evolution, without an intermediate steepening. It should also be pointed out that although the above classification is somewhat arbitrary, the above conclusion is not changed even if the age groups are made differently.

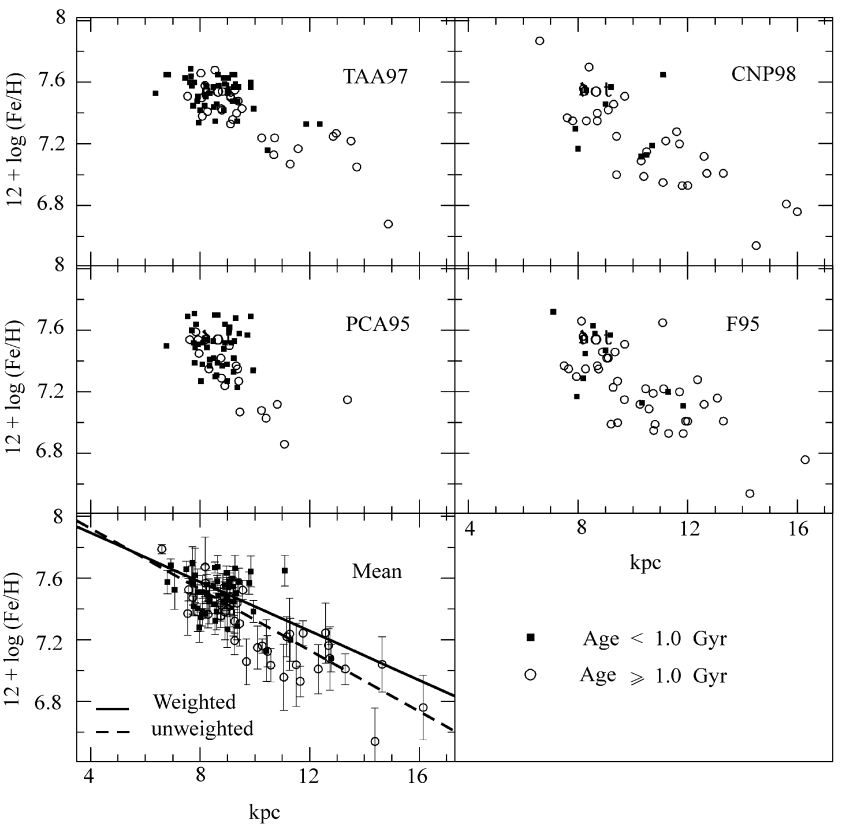

Fig. 4 Abundance gradient of open clusters for the combined sample and the four original samples. The dash line is the unweighted least square fitting of the data. The resulted gradient for the new sample is -0.099 ± 0.008 dex kpc^{-1}. The full line for the weighted fitting gives the value -0.080 ± 0.001 dex kpc^{-1}.

4 MODEL PREDICTION AND COMPARISON

4.1 Basic Model and Iron Gradient Evolution

As mentioned in the Introduction, current model predictions for the gradient evolution do not converge. Some predict a steepening of the gradient with time, while others predict just the opposite. A time flattening evolution was also suggested by our latest Galactic chemical

evolution model. The details are presented in Boissier & Prantzos (1999) (hereafter BP1999), and Hou et al. (2000) (hereafter HPB2000). Here we just recall some of the main points of the model.

The galactic disk is simulated as an ensemble of concentric, independently evolving rings, gradually built up by infall of primordial composition. The assumption of infall is traditionally based upon the requirement to explain the locally observed metallicity distribution of long-lived stars, which cannot be explained by the simple "closed-box" model (leading to the well-known "G-dwarf problem"), and it is also the basic assumption for nearly all Galactic chemical evolution model.

We have utilized the metallicity-dependent yields from Woosley and Weaver (1995) for intermediate mass elements. Iron-producing SNIa are included, their rate being calculated with the prescription of Matteucci and Greggio (1986). We also adopt the recent yields of SNIa from the exploding Chandrashekhar-mass CO white dwarf models W7 and W70 of Iwamoto et al. (1999) in order to account for the additional source of Fe-peak elements, required to explain the observed decline of O/Fe abundance ratio in the disk (Goswami & Prantzos 2000). The adopted stellar Initial Mass Function (IMF) is a multi-slope power-law between 0.1 $M_{\odot}$ and 100 $M_{\odot}$ from the work of Kroupa et al. (1993). The star formation rate (SFR) is locally given by a Schmidt-type law, i.e., proportional to some power of the gas surface density $\Sigma_{\rm g}$: $\Psi \propto \Sigma_{\rm g}^{1.5}$, according to the observations of Kennicutt (1998). It varies with galactocentric radius R, as:

$$\Psi(t,R) = \alpha \Sigma_{\rm g}(t,R)^{1.5}\ V(R)\ R^{-1}, \tag{1}$$

where $V(R)$ is the circular velocity at radius R. This radial dependence of the SFR was suggested by the theory of star formation induced by density waves in spiral galaxies (e.g., Wyse & Silk 1989). The efficiency of the SFR α in the above equation is fixed by the requirement that the local gas fraction $\sigma_{\rm g}(R_0) \sim 0.2$, is reproduced at $T = 13.5\,$Gyr, which is the adopted age of the Galactic disk.

The infall rate is assumed to be exponentially decreasing in time with a characteristic time τ. In the solar neighborhood we adopted $\tau = 7\,$Gyr in order to reproduce the local G-dwarf metallicity distribution, and τ is assumed to increase outwards, thus mimicking the "inside-out" formation of galactic disk (see details in BP1999, HPB2000). Note that there are other forms of infall rate, such as Gaussian, two-component (thick and thin disk, see Chang et al. 1999, Chiappini et al. 1997), but they are eventually similar after evolving for a long time.

Our model presented above can well account for the evolution of the solar neighborhood as well as for the whole disk (see BP1999, HPB2000). We have calculated the evolution of the abundance for all elements between H and Zn. In HPB2000, we present the main results for elements H, C, N, O, Ne, Mg, Al, Si, S and Ar, which have observational data from nebula and early B stars available for a comparison. We will concentrate in this paper on the evolution of the iron abundance, based on the observational data from open clusters.

Figure 5 presents the results for the radial profile of iron abundance (upper panel) and the evolution of iron gradient (lower panel). It shows that the final value (at $T = 13.5\,$Gyr) of the iron abundance at $R_0 = 8\,$kpc is the solar value. The final abundance profile ($T = 13.5\,$Gyr) is flatter in the inner disk. As already described in Prantzos and Aubert (1995), this could be due to the fact that in those regions large populations of low-mass, long-lived stars that were formed early in galactic history which ejected a lot of metal-poor gas at the end of their evolution, so diluting the metal abundances; this effect was absent in the outer regions which lack very old stellar populations.

Another feature of the model is the prediction that the abundance gradients flatten with time. This seems a natural result of models of "inside-out" formation of the galactic disk. Indeed, in the inner parts of the disk, there is a rapid increase of the metal abundance at early times and soon leading to a maximum gas metallicity which then remains constant or decreases due to the gas dilution by the dying stars. As time goes on, star formation "migrates" to the outer disk, produces metals there and flattens the abundance gradient. Recent data from planetary nebula give an average gradient flattening rate about -0.004 dex kpc^{-1} Gyr^{-1}(Maciel 2002), in remarkable agreement with our model prediction.

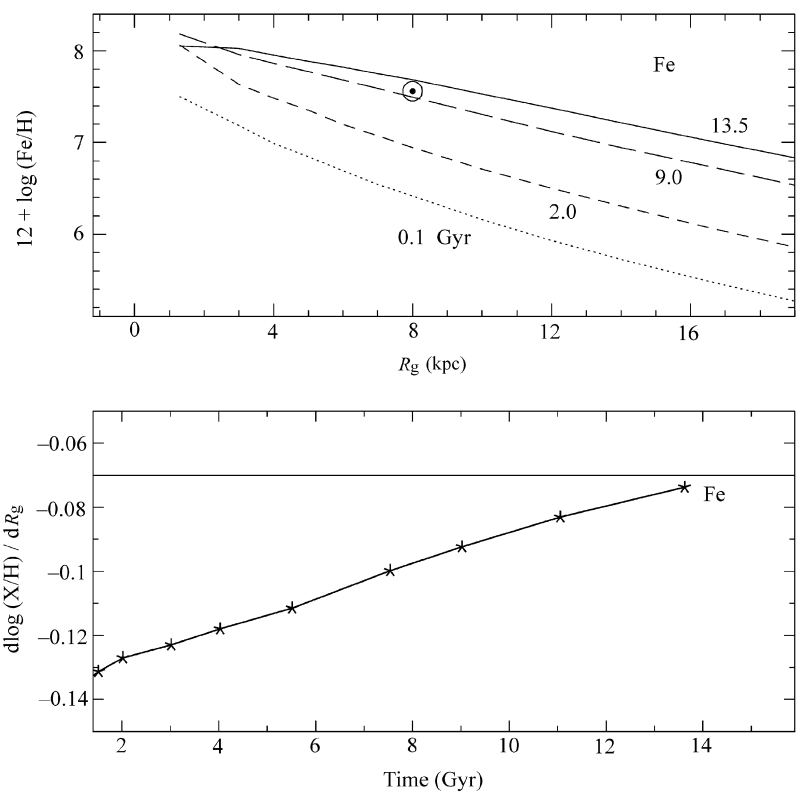

Fig. 5 Radial profile of iron abundance (upper panel) at four evolution times and the gradient evolution (lower panel, expressed in dex kpc^{-1}, range: $4-14$ kpc from the center) in the Milky Way disk, in the framework of the model presented in Sect. 4. The predicted current iron gradient is about -0.072 dex kpc^{-1}. From this figure, we see that the gradient was steeper in the past.

We notice, however, that our picture is just the opposite of that of Chiappini et al. (1997, 2001). Their models, which also adopt a simulated "inside-out" disk formation scenario, predict a time steepening behavior for the gradient evolution. The main reason could be that they adopted a threshold density in the star formation process during both the halo and disk phases (Chiappini et al. 2001). In such a case, at early epochs, due to the large amount of primordial

infalling gas, the efficiency of the chemical enrichment of the inner parts of disk was low, leading to a flat initial abundance gradient. Then, at later epochs, while the SFR was still much higher in the inner disk than in the outer regions, the infall of metal poor gas was stronger in the outer than in the inner part, thus steepening the gradients.

In a recent work, Chang et al. (2001) pointed out that the gradient evolution with time should not be described simply by "steepening" or "flattening" as suggested by Hou et al. (2000) and Chiappini et al. (2001). Their model prediction shows that both the absolute value and evolution of the abundance gradients may be different in the inner and outer regions, and strongly depend on the chemical composition of the infall material, which is strictly related to the mechanism of Galaxy formation, including the formation of halo.

While several scenarios are possible on the basis of chemical evolution model, only one of the alternatives should be the real one during the formation and evolution of the Milky Way disk. This question could, in principle, be answered by a comparison to available observations, particularly to open clusters and planetary nebula data. A detailed comparison to open clusters now follows.

4.2 Comparison to Open Clusters Gradients

As mentioned in Section 3, a meaningful comparison could only be done by dividing open clusters into sub-groups according to their ages. Such a comparison is presented in Fig. 6. We select young open clusters with ages less than 1.0 Gyr, intermediate objects with ages between 1.0 and 4.5 Gyr, and older clusters with ages greater than 4.5 Gyr. We also plot the model results for each group.

Least-square fitting for the three groups results in the three gradients –0.055, –0.095 and –0.108 dex kpc^{-1} for the young, intermediate and old clusters. They show the same trend as our model predictions (see Figure 5). However, the scatter in the observed data are much larger than the values given by the model (shaded area in Figure 6) for all galactocentric distances, especially for young clusters. Further examination of Figure 6 shows that:

(1) The fitted gradient for young clusters is less than that of the model prediction. Young clusters are heavily concentrated in the solar neighborhood due to the preferential destruction of the inner-disk open clusters. It has long been recognized that frequent encounters with giant molecular clouds, which are found primarily in the inner Galaxy, are very effective at destroying typical open clusters. In contrast, the outer disk strongly favors cluster longevity, which results in the outer clusters being predominantly older. Therefore, it is particularly important to measure the iron abundance by observing the B-type stars in distant young clusters or associations.

(2) For intermediate and old cluster groups, our model predictions are compatible with the observations. In fact, the difference of observed abundance radial profile between older and intermediate clusters is small considering the large uncertainties in both the age and distance determinations. However, the existence of a steeper gradient for the older clusters is clear; there is a decrease in metallicity with increasing Galactocentric distance. It is also clear that there exists metal-rich clusters with ages up to 8 Gyr. This suggests that the Galactic disk must has undergone very rapid, inhomogeneous enrichment (infall playing an important role, see Chang et al. 2001) to produce the substantial dispersion at all ages and locations in the disk. This point is also supported by the fact that cluster metallicity is not a function of age when the cluster abundances are corrected for the radial abundance gradient and reduced to the values the clusters would have at the solar position (Friel 1995, Ying 1998). This indicates that the

cluster abundance is controlled primarily by where, and not by when, the cluster was formed. Looking over the three panels in Figure 6, it is clear that over the whole age of the disk and at any position in the disk, the oldest clusters may have formed with compositions similar to, and as enriched as those of the young or intermediate age objects.

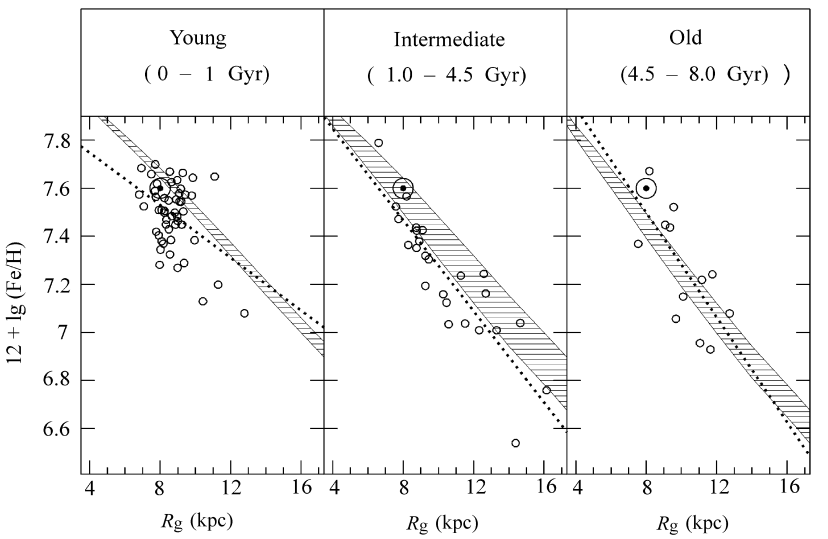

Fig. 6 Gradient evolution from open clusters and model predictions. From left to right, profiles are shown for young, intermediate and old objects. The corresponding model results are shown at time $T = 12.5-13.5$ Gyr or age $= 0.0-1$ Gyr (left column, shaded area), at $T = 9.0-12.5$ Gyr or age $= 1.0-4.5$ Gyr (middle column, shaded area), and at $T = 5.5-9.0$ Gyr or age $= 4.5-8.0$ Gyr (right column, shaded area). Dotted lines are the unweighted least square fitting for the data. The fitted gradients are -0.055, -0.095, -0.109 dex kpc^{-1} for the young, intermediate and old groups, respectively.

By adopting a star formation rate that varies with the gas mass, galactocentric distance and an infall law with a distance-dependent time scale, thus mimicking the "inside-out" scenario, our model predicts well a steeper gradient at early epoch of the disk evolution. Also, the model predicts that the gradient evolves with time and flattens as the disk evolves.

Since young clusters are mostly biased in the solar vicinity, it is more reliable to adopt abundance data from nebulae (HII regions, early B stars) as gradient tracers for the young disk. The available observations give a gradient of the order of -0.07 dex kpc^{-1} for the typical element O (Smartt & Rolleston 1997, HPB2000). Taken together with older cluster data, these results indicate that the abundance gradient in the disk has changed very slowly over its lifetime. However, we should be careful when comparing the results between cluster metallicities and nebula oxygen abundances. Iron is produced mainly in SNIa and as such has had a distinctly different evolutionary history in the Galaxy (Edvardsson et al. 1993) as compared to oxygen which has its origin in SNII. They may be somewhat different in nature.

5 SUMMARY

Based on four open cluster samples, we compiled a new sample of clusters. From the combined sample, we made a detailed analysis of the iron gradient along the Galactic disk and its evolution with time. We also presented our model predictions on the current iron gradient and its time evolution. The predictions are then compared with the open clusters data. The main results are summarized as follows:

(1) The iron radial gradient from open clusters is about -0.099 ± 0.008 dex kpc^{-1} based on the whole sample, which is rather larger than the most recent determination of oxygen gradient in nebulae and young stars. However, the ages of some clusters used are up to 8 Gyr old, hence they are not at all representative of the present disk as sampled by young objects. The fact that the magnitude of the Fe gradient as sampled by these old stars is so similar to that from present day O gradient is quite surprising, and the way that they relate to each other is still unclear.

(2) By dividing clusters into age groups, we show that the iron gradient was steeper in the past and that it evolved slowly with time. Although statistically this conclusion is not very significant, it shows a trend which should be verified with a much larger sample.

(3) Our chemical evolution model predicts a steady flattening of the Fe gradient with time, due to the adopted "inside-out" formation scenario of the Galactic disk. Such an evolution is also found in other work using similar assumptions. However, there are also models that predict the opposite behavior for the gradient evolution. Future work should aim at finding a present day iron abundance gradient through young stars or an oxygen gradient in old disk stars in order to clarify these two evolutionary trends.

How the abundance gradient evolves along the Galactic disk remains one of the unsettled issues concerning the formation and evolution of the Milky Way disk. Open clusters and planetary nebulae are two most useful observational tracers here. Much more precise determinations of the ages, distances, and metallicities for those objects would be required. Theoretically, the recent model of Chang et al. (2001) pointed out that the gradient along the Galactic disk cannot be described by a single value and the time evolution cannot be described only by the words "steepening" or "flattening". A single linear value of gradient strongly depends on the way of calculation. And the gradient evolution is not only dependent on the adopted forms of SFR and infall rate, but is also heavily affected by the chemical composition of the infalling gas. Therefore, it is necessary to clarify which assumption plays the central role in shaping the evolution trend in the current chemical evolution models.

Acknowledgements J. L. Hou acknowledges the warm hospitality of IAP (Paris) where part of the work was done. The authors also thank Dr. N. Prantzos, Prof. Wang J. J. for their helpful discussion. The authors also thank the comments from anonymous referee(s) which improve the paper. This research was supported partly by the National Natural Science Foundation of China (No. 19873014) and NKBRSFG19990754, and partly by SRF for ROCS, SEM.

References

Allen C., Carigi L., Peimbert M., 1998, ApJ, 494, 247
Boissier S., Pranzos N., 1999, MNRAS, 307, 857 (BP1999)

Bragaglia A., Tosi M., Marconi G. et al., 2000, In: F. Giovannelli, F. Matteucci eds., "The chemical evolution of the Milky Way: stars versus clusters", Kluwer, in press (astro-ph/9912130)
Brown J. A., Wallerstein G., Geisler D. et al., 1996, AJ, 112, 1551
Cameron L. M., 1985, A&A, 147, 47
Carraro G., Ng Y. K., Portinari L., 1998, MNRAS, 296, 1045 (CNP98)
Chang R. X., Shu C. G., Hou J. L. et al., 2001, Chin. J. Astron. Astrophys., submitted
Chang R. X., Hou J. L., Shu C. G. et al., 1999, A&A, 350, 38
Chen Y. Q., Nissen P. E., Zhao G. et al., 2000, A&AS, 141, 491
Chiappini C., Matteucci F., Gratton R., 1997, ApJ, 477, 765
Chiappini C., Matteucci F., Romano D., 2001, ApJ, 550, 1044
Corder S., Twarog B. A., 2001, AJ, 122, 895
Cui C. Z., Zhao G., Zhao Y. H. et al., 2000, Science in China (series A), 30, 953
Edvardsson B., Andersen J., Gustafsson B. et al., 1993, A&A, 275, 101
Friel E. D., 1999, Ap&SS, 265, 271
Friel E. D., 1995, ARA&A, 33, 381 (F95)
Friel E. D., Janes K.A., 1993, A&A, 267, 75 (FJ93)
Goswami A., Prantzos N., 2000, A&A, 359, 191
Henry R. B. C., Worthey G., 1999, PASP, 111, 919
Hou J. L., Chang R. X., 2001, Progress in Astronomy, 19(1), 68
Hou J. L., Prantzos N., Boissier S., 2000, A&A, 362, 921 (HPB2000)
Iwamoto K., Brachwitz F., Nomoto K. et al., 1999, ApJS, 125, 439
Janes K. A., 1979, ApJS, 39, 135
Janes K. A., Phelps R. L., 1994, AJ, 108, 1773
Janes K. A., Tilley C., Lynga G., 1988, AJ, 95, 771
Kennicutt R. C. Jr., 1998, ApJ, 498, 541
Kilian-Montenbruck J., Gehren T., Nissen P. E., 1994, A&A, 291, 757
Kroupa P., Tout C., Gilmore G., 1993, MNRAS, 262, 545
Lyngå G., 1987, Catalogue of Open Cluster Data, distributed by Centre de Donnes Stellaires (CDS), Strasbourg, France
Maciel W. J., Köppen J., 1994, A&A, 282, 436
Maciel W. J., Quireza C., 1999, A&A, 345, 629
Maciel W. J., Costa R. D. D., 2002, IAU Symp. 209, 2002, in press (astro-ph/0112210)
Matteucci F., Greggio L., 1986, A&A, 154, 279
Mollá M., Ferrini F., Diaz A.I., 1997, ApJ, 475, 519
Panagia N., Tosi M., 1981, A&A, 96, 306
Piatti A., Claria J. J., Abadi M. G., 1995, AJ, 110, 2813 (PCA95)
Piatti A., Claria J. J., Minniti D., 1993, JAp&A, 14, 145
Portinari L., Chiosi C., 1999, A&A, 350, 827
Prantzos N., Aubert O., 1995, A&A, 302, 69
Rolleston W. R. J., Brown P. J. F., Dufton P. L. et al., 1993, A&A, 270, 107
Samland M., Hensler G., Theis Ch., 1997, ApJ, 476, 544
Simpson J. P., Colgan S. W. J., Rubin R.H. et al., 1995, ApJ, 444, 721
Smartt S. J., 2000, In: F. Giovannelli, F. Matteucci eds., "The chemical evolution of the Milky Way: stars versus clusters", Kluwer, in press
Smartt S. J., Rolleston W. R. J., 1997, ApJL, 481, 47
Thogersen E. N., Friel E. D., Fallon B. V., 1993, PASP, 105, 1253
Tosi M., 2000, In: F. Giovannelli, F. Matteucci eds., "The chemical evolution of the Milky Way: stars versus clusters", Kluwer, in press (astro-ph/9912370)
Tosi M., 1988, A&A, 197, 47
Twarog B. A., Ashman K. A., Anthony-Twarog B. J., 1997, AJ, 114, 2556 (TAA97)
Woosley S. E., Weaver T. A., 1995, ApJS, 101, 181
Wyse R., Silk J., 1989, ApJ, 339, 700
Ying Xiao, 1998, Thesis, Shanghai Astronomical Observatory